ANALYSIS OF THE ATTITUDE MOTION AND CROSS-SECTIONAL AREA OF TIANGONG-1 DURING ITS UNCONTROLLED RE-ENTRY

S. Sommer, V. Karamanavis, F. Schlichthaber, T. Patzelt, J. Rosebrock, D. Cerutti-Maori, and L. Leushacke

Fraunhofer Institute for High Frequency Physics and Radar Techniques FHR, 53343 Wachtberg, Germany, Email: {svenja.sommer, vasileios.karamanavis, frank.schlichthaber, thomas.patzelt, jens.rosebrock, delphine.cerutti-maori, ludger.leushacke}@fhr.fraunhofer.de

ABSTRACT

The Chinese space station TIANGONG-1 re-entered the Earth's atmosphere on 2 April 2018 in an uncontrolled fashion. The progress of the re-entry was monitored with the Tracking and Imaging Radar (TIRA) and radar data was generated for tracking and imaging purposes. Additionally to highly precise orbit parameters for re-entry forecasting and high resolution radar images for status analysis, the intrinsic rotation parameters for 24 passes during different stages of the re-entry process were estimated. The data shows that the rotation velocity increased significantly with decreasing altitude. The rotation velocity at a perigee height of 345 km was 0.18°/s and accelerated to 3.6°/s at 161 km. Furthermore, the cross-sectional area for different passes were derived from the data in conjunction with a model, indicating that the effective cross-sectional area decreased from about 65 m^2 to about 26 m^2 based on a model derived from radar data.

Keywords: TIRA, re-entry, Tiangong-1, cross-sectional area, rotation.

1. INTRODUCTION

The likely uncontrolled Chinese space station TIANGONG-1 re-entered the Earth's atmosphere on 2 April 2018. The descent was monitored using TIRA (Tracking and Imaging Radar), the space observation radar operated by the Fraunhofer Institute for High Frequency Physics and Radar Techniques FHR in Wachtberg, Germany. Data for re-entry forecasting for the German Space Situational Awareness Center were collected with TIRA. In addition, the attitude behavior of a re-entering spacecraft was systematically analysed for the first time.

Forecasting the re-entry date and location is difficult as the accuracy of the re-entry predictions depends on several factors. Atmospheric drag has a detrimental effect to the remaining life time of a spacecraft. The drag depends on several components, such as atmospheric density, attitude of the spacecraft, its shape and surface material. Some are often known, such as shape and surface material. The atmospheric density, however, is highly variable and influenced by the solar activity and other space weather conditions. Furthermore, the attitude motion behaviour of the object is usually unknown, rendering the cross-sectional area unknown as well. Hence, the drag area, needed for forecasting, is unknown. The knowledge of, at least, the current cross-sectional area might help to improve re-entry forecasting.

Radar measurements can be used to derive the attitude motion of spacecraft [4, 5]. A series of radar images can be generated using the inverse synthetic aperture radar (ISAR) principle. In this configuration, the radar is considered stationary while the object's rotation (apparent or real) is used to generate each radar image. The image scaling along cross-range (perpendicular to range) depends on the velocity of the apparent rotation. The rotation vector needs therefore to be known a priori to scale the ISAR image correctly in cross-range. On the other hand, the ISAR images should also be used to derive the rotation vector. To overcome this problem, a model of the spacecraft is used and fitted to a series of ISAR images. The rotation vector can then be determined using a maximum-likelihood approach to estimate the rotation vector and scale the ISAR images correctly.

TIANGONG-1 was regularly monitored during its re-entry starting in February 2017 for a first rotation analysis until the last observable pass for TIRA on 1 April 2018. In total, 24 passes were monitored and the rotation vector determined. Limited information was available on TIANGONG-1, especially regarding its dimensions. Therefore, the size of the main body and solar panels, needed for the analysis, had been derived from ISAR images. The derived model consist of a cylindrical main body with a length of 9.3 m and a diameter of 2.2 m. Two rectangular solar panels are attached to either side of the main body, each with dimensions of 7 m x 2.8 m.

2. DERIVING THE ROTATION VECTOR FROM ISAR IMAGES

The radar images are generated using the TIRA system, located in Wachtberg, Germany (50.6° N, 7.1° E). It utilizes a narrowband radar in L-band for tracking purposes and a broadband K_u-band radar for imaging. The images used in this analysis were obtained by the K_u-band radar that operates at a center frequency of 16.7 GHz with circular polarization. For further details, see [2].

The method to derive the rotation vector from a series of ISAR images is described in [4]. For completeness, it is shortly discussed here.

While radar excels at delivering the range to a target, imaging an object requires further information perpendicular to range, the so called cross-range. The cross-range information can be gained by exploiting the relative motion between radar and object. The radar is assumed stationary on the Earth's surface while the object passes over the radar. This motion can be divided in two components: a translational motion, due to the spacecraft orbital motion and a rotational motion. The line of sight vector relative to the reference frame fixed on the satellite varies, depending on Earth rotation, the translational motion but also due to a possible intrinsic rotation of the space object. This leads to changes in the relative distance of object points between consecutive pulses and results in corresponding phase changes and is used to infer the cross-range information. The range and cross-range directions span the image plane of an ISAR image. The rotation velocity scales the cross-range. Hence, it must be known a priori to scale the ISAR images correctly. Although Earth rotation, object orbit and radar location are well known, the intrinsic rotation of the space object usually is not, so the object's attitude cannot be estimated directly from its attitude relative to the image plane. This problem can be solved by employing a model, with known dimensions, of the space object. It is manually adapted for a set of ISAR images that its projection matches the ISAR images with incorrect cross-range scaling. After that, a rotation vector can be estimated that fits the assigned models best under the assumption, so that the rotation vector in ECI coordinates, *J2000*, is virtually constant for the duration of the pass and the ISAR images can be scaled correctly.

The ISAR image is a 2D image of a 3D object. This leads to the effect, that two orientations of a symmetric spacecraft can be represented by the same ISAR image, i.e. the object is mirrored on the image plane. This leads to two possible rotation vectors for each image,

$$\begin{pmatrix} \omega_{2,1} \\ 0 \\ \omega_{2,3} \end{pmatrix} = \begin{pmatrix} -\omega_{1,1} \\ 0 \\ \omega_{1,3} \end{pmatrix}, \tag{1}$$

where $\omega_\mathbf{1}$ and $\omega_\mathbf{2}$ are a set of mirrored rotation vectors relative to and in image coordinates and the second component points in cross-range direction. The third coordinate points orthogonal to the image plane. This may lead, under certain conditions, to two different solutions in ECI coordinates that can represent the object motion during one pass. The rotation vector was selected based on the smoothness and continuity of the data set. That means, that the evolution of the rotation vector sequence of all analysed passes should not jump or change direction drastically with time in all considered coordinate systems, i.e. the temporal evolution should be smooth.

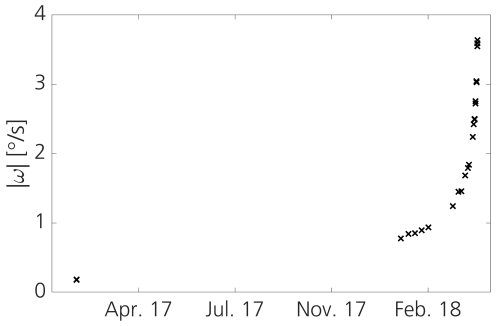

Figure 1. Rotation velocity of TIANGONG-1 versus time.

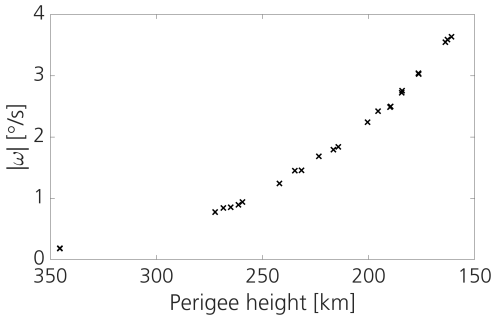

Figure 2. Rotation velocity of TIANGONG-1 versus perigee height.

3. RESULTS

3.1. Rotation velocity

The rotation velocity is the norm of the rotation vector. The temporal evolution of the rotation velocity of TIANGONG-1 is shown in Fig. 1. The first two observations were conducted on 9 February 2017. The observations continued in January 2018. TIANGONG-1 was rotating with 0.18°/s in February 2017 which increased to 3.6°/s at the last observed pass on 1 April 2018. As the rotation becomes faster with decreasing altitude, a connection with the evolution of atmospheric parameters could be possible. Figure 2 shows the rotation velocity over perigee altitude. It can be clearly noted that the rotation velocity does not increase linearly with decreasing altitude.

3.2. Rotation axis and cross-sectional area

The sequence of the full rotation vectors is shown in Fig. 3. As seen before in the rotation velocity over time plots, the vector length increases with time. Furthermore, it

can be seen that the rotation axes in ECI coordinates lie roughly in a plane and the rotation axes describe nearly a half circle over time.
It is not only interesting how TIANGONG-1 moved in an inertial coordinate system but in order to describe the rotation behavior completely, the rotation axis of the spacecraft itself needs to be considered. The normalized rotation axes of TIANGONG-1 with respect to the spacecraft's body is shown in Fig. 4. Except for two observations in February 2017, all rotation axes point approximately in the same direction. This indicates, that the rotation axis of the spacecraft itself did not change during the last months prior to re-entry. Furthermore, the rotation axes are perpendicular to the solar panel plane and probably along a principal axis of inertia. However, this remains unclear as the mass distribution is unknown.
If the rotation vector together with the initial attitude is known, the cross-sectional area can be derived. This way, the instantaneous attitude can be derived and the instantaneous cross-sectional area calculated. This assumes, that the model dimensions are correct and that possible extensions can be neglected. It should be noted, that the rotation axis is considered to be fixed in an inertial coordinate system and therefore changes in an orbit coordinate system over time. The cross-sectional area is considered the area that is oriented normal to the flight direction. The estimated cross-sectional areas for three passes are shown in Fig. 5, for a pass at the start of the observation series, in February 2018 at the middle and the last observed pass on 1 April 2018. It can be seen for all three passes, that the cross-sectional area changes with time. The changes are faster for later passes which is in accordance with the increased rotation velocity. As the cross-sectional area changes during the pass, the average cross-sectional area is indicated by a dashed line for each pass. It can be noted that the average cross-sectional area decreased over time which might be a result of the atmospheric drag. For the pass on 9 February 2017, the estimated averaged cross-sectional area was 60 m^2, in 11 February 2018 40 m^2 and 26 m^2 on 1 April 2018. Due to the low rotation velocity compared to the observation time, for the passes on 9 February 2017 and 11 February 2018, only a part of a revolution was observed. Hence, the averaged cross-sectional areas do not necessarily represent the averaged cross-sectional area of a full revolution. An extrapolation could be used to estimate the averaged cross-sectional area for a full revolution, as the orbit, rotation vector and initial attitude are known, under the assumption, that the rotation vector does not change remarkably within one revolution.

4. DISCUSSION

Only scarcely detailed information on the rotation of spacecraft during re-entry can be found in the literature. Typically, the rotational behavior below 150 km is studied in detail [3, 1] with no consideration of rotation above that altitude. In this case study, the rotation of an uncontrolled spacecraft starts to accelerate above that altitude and already reached 3.6°/s in 160 km perigee height. Al-

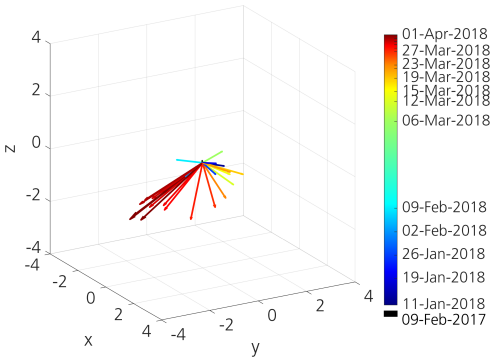

Figure 3. Rotation vectors of TIANGONG-1 in ECI coordinates. The time is color coded.

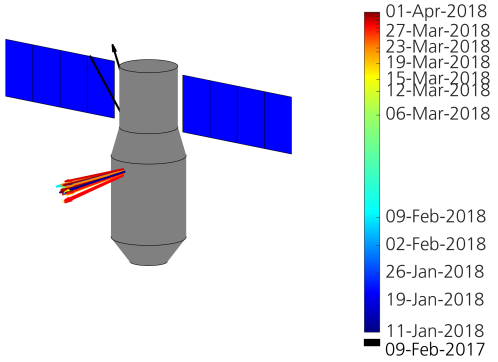

Figure 4. Rotation axis of TIANGONG-1 in model coordinates. The time is color coded.

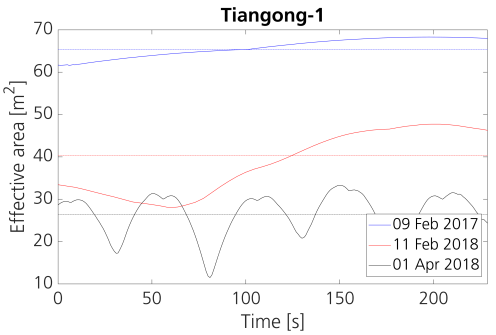

Figure 5. Cross-sectional areas of TIANGONG-1 during three different passes. The solid lines indicate the cross-sectional area versus time, color coded for each pass. The dashed lines indicate the respective averaged cross-sectional areas for each pass.

though the atmosphere is not as dense as in lower altitudes, it appears that this is sufficient enough to accelerate the intrinsic rotation with increasing atmospheric density. The atmosphere does not only accelerate the rotation velocity but also seems to influence the rotation axis. The decrease of the averaged cross-sectional area of the three passes could be attributed to aerodynamic alignment. This conclusion is based only on three passes and need further investigation in the future. Additionally, the estimation of the cross-sectional area is based on a model derived from ISAR images and might not represent the actual dimensions of TIANGONG-1, leading to errors. Furthermore, the rotation analysis is based on the assumption, that the rotation vector is constant in an inertial frame of reference for a pass. This assumption holds for this study, as a reasonable rotation vector could be derived for each pass. However, the rotation vector is only assumed constant for each pass and can change after the observation. Another source of error is the fitting of the model to the ISAR images for the rotation vector estimation. As mentioned before, the model itself can contain errors, as well as the fitting of the model to the images. A longer series of ISAR images reduces this error, hence, the length of the ISAR images series influences the uncertainty of the rotation vector estimations. Additionally, the method used in this study leads to two rotation vectors. The selection of the correct rotation vector is based here on the smoothness of the temporal evolution in ECI, perifocal and model coordinates. If a sudden change in rotation axis orientation occurs, it might be misinterpreted. In the future, a suitable method should be developed for deriving the correct rotation vector unambiguously.
This study shows that radar data can be used to derive the rotation vector and cross-sectional area of a re-entering spacecraft. As the accuracy of re-entry forecast depends on knowledge about the atmospheric drag, this method can be used to derive either the instantaneous or average cross-sectional area of the spacecraft to calculate the atmospheric drag. Furthermore, the increase in rotation velocity might also help to understand the interaction between re-entering spacecraft and atmosphere better.

5. SUMMARY

This study used radar data from the TIRA system of TIANGONG-1 to derive the vectorial rotation and cross-sectional area during its re-entry in a systematical approach. It was shown that the rotation velocity increased significantly already above 150 km. The increase in rotation velocity did not depend linearly on the altitude.
Furthermore, the cross-sectional area of TIANGONG-1 was derived and a decrease in estimated cross-sectional area from 65 m^2 to 26 m^2.
The knowledge of the cross-sectional area might help to improve re-entry forecasts in the future by providing timely estimates of the cross-sectional area.

ACKNOWLEDGMENTS

Measurements for this study have been partly commissioned and financed by the German Space Situational Awareness Center and partly by the European Space Agency. The authors would like to thank N. Daalmanns, G. Mueller, R. Perkuhn, F. Rustemeier and H. Wotzke for conducting the measurements and A. Dieser, M. Heinrichs, R. Frank, J. Marnitz and G. Schumacher for technical support.

REFERENCES

1. Patrick Gallais. *Atmospheric Re-Entry Vehicle Mechanics*. Springer, 2007.
2. D. Mehrholz. Ein Verfolgungs- und Abbildungsradarsystem zur Beobachtung von Weltraumobjekten. *Frequenz*, 50:138–146, July 1996.
3. Frank J. Regan and Satya M. Anandakrishnan. *Dynamics of Atmospheric Re-Entry*. AIAA Education Series, 1993.
4. J. Rosebrock. Absolute attitude from monostatic radar measurements of rotating objects. *IEEE Transactions on Geoscience and Remote Sensing*, 49(10):3737–3744, October 2011.
5. S. Sommer, J. Rosebrock, D. Cerutti-Maori, and L. Leushacke. TEMPORAL ANALYSIS OF ENVISAT'S ROTATIONAL MOTION. *JBIS*, 70:45–51, 2017.